Journal of Radiotherapy in Practice

Journal of Radiotherapy in Practice (2009)
8, 185–194

doi:10.1017/S1460396909990240

Original Article

Evaluation on lung cancer patients' adaptive planning of TomoTherapy utilising radiobiological measures and Planned Adaptive module

Fan-Chi Su[1], Chengyu Shi[2], Panayiotis Mavroidis[3,4], Prema Rassiah-Szegedi[5], Niko Papanikolaou[2]

[1]*Radiation Oncology Department, Cancer Therapy and Research Center, San Antonio, Texas, USA,* [2]*Division of Radiological Sciences, University of Texas Health Science Center at San Antonio, San Antonio, Texas, USA,* [3]*Department of Medical Radiation Physics, Karolinska Institute and Stockholm University, Sweden,* [4]*Department of Medical Physics, Larissa University Hospital, Larissa, Greece,* [5]*Department of Radiation Oncology, University of Utah, Salt Lake City, Utah, USA*

Abstract

Adaptive radiation therapy is a promising concept that allows individualised, dynamic treatment planning based on feedback of measurements. The TomoTherapy Planned Adaptive application, integrated to the helical TomoTherapy planning system, enables calculation of actual dose delivered to the patient for each treatment fraction according to the pretreatment megavoltage computed tomography (MVCT) scan and image registration. As a result, new fractionation treatment plans are available if correction is necessary. In order to evaluate the real clinical effect, biological dose is preferred to physical dose. A biological parameter, biologically effective uniform dose ($\overline{\overline{D}}$), has the advantages of not only reporting delivered dose but also facilitating the analysis of dose–response relations, which link radiation dose to the clinical effect. Therefore, in this study, four lung patients' adaptive plans were evaluated using the $\overline{\overline{D}}$ in addition to physical doses estimated from the TomoTherapy Planned Adaptive module. Higher complication-free tumour control probability (P_+) (of about 8%) was observed in patients treated with larger dose-per-fraction by using the $\overline{\overline{D}}$ in addition to the physical dose. Moreover, a significant increase of 13.2% in the P_+ for the adaptive TomoTherapy plan in one of the lung cancer patients was also observed, which indicates the clinical benefit of adaptive TomoTherapy.

Keywords

Biologically effective uniform dose; adaptive radiotherapy; helical TomoTherapy; treatment planning; radiobiological objectives

INTRODUCTION

Helical TomoTherapy is a feasible solution of image-guided radiation therapy to fulfil highly conformal intensity-modulated radiotherapy (IMRT).[1,2] The presence of the integrated

Correspondence to: Chengyu Shi, Division of Radiological Sciences, University of Texas Health Science Center at San Antonio, San Antonio, Texas, USA. E-mail: shic@uthscsa.edu

online megavoltage computed tomography (MVCT) unit results in innovative approaches to adaptive radiation therapy.[2] Adaptive radiation therapy is a concept/technique to modify radiation treatments in a closed-loop process, utilising a systematic feedback of measurements.[3] MVCT, which would be acquired just before each treatment, enables verification of daily set-up and corrections for internal organ motion. These MVCTs also serve as inputs for the adaptive module of helical TomoTherapy, the Planned Adaptive software.

The Planned Adaptive software is capable of registering manually and automatically the MVCT images generated on the day of the treatment with the kilovoltage computed tomography (kVCT) images used for treatment planning.[4] With the image registration, the volume changes in the target and/or in the normal tissues during the treatment course of TomoTherapy could be evaluated.[4–6] Based on the registered kVCT-MVCT images, a verification dose distribution is calculated to indicate the actual dose delivered to the target and the adjacent normal tissues.[7] Using the verification doses and sinograms from different treatment fractions, a summation dose is generated for the partial or the whole course of treatment. Based on the dose deviation of the summation dose from the planned prescription, the adaptive modification of the rest treatment fractions could subsequently be made.[4,6,8] Although adaptive planning is considered to be a promising way to continuously adjust the dose that would be delivered to the target and organs at risk, the clinical benefit in relation to the cost of extra time and effort of re-planning remains mostly unproven.

Biologically effective uniform dose ($\overline{\overline{D}}$) is able to report physical dose delivery, but more importantly, it facilitates the analysis of dose-response relations, which link the radiation dose to the clinical effect.[9] Therefore, the concept of the $\overline{\overline{D}}$ has been used to assess the difference between planned and delivered IMRT dose distributions.[10] Previous studies have utilised $\overline{\overline{D}}$ for plan comparison between helical TomoTherapy and multileaf collimator–based IMRT.[11,12]

With the ability to retrospectively review the delivered doses to the target and critical organs by using the Planned Adaptive software plus the capability of converting the physical doses to clinical effectiveness using the $\overline{\overline{D}}$, the goal of this study is to predict the radiobiological effects of the adaptive TomoTherapy using the $\overline{\overline{D}}$ in addition to physical dose indices (such as the dose-volume histogram (DVH) and the mean dose). Furthermore, the clinical impact of the adaptive plans in TomoTherapy would be assessed by using the $\overline{\overline{D}}$ and the complication-free tumour control probability, P_+.

MATERIALS AND METHODS

Study candidates and adaptive software module of TomoTherapy

Helical TomoTherapy was delivered using the Hi-Art TomoTherapy unit (TomoTherapy Inc., Madison, WI). Four lung cancer patients who underwent helical TomoTherapy were randomly selected retrospectively. The general information of these four patients is listed in Table 1. Patient 4 had the original treatment plan for 16 fractions followed by the second-phase treatment plan for the remaining 9 fractions. Daily MVCT scans were performed and registered with the planning kVCT images to correct the patient set-up and internal organ motions. Evaluation of the delivered dose distribution in each treatment fraction of the TomoTherapy was performed by using the Planned Adaptive software (TomoTherapy Inc., Madison, WI).

Before the assessment of the delivered dose distribution for each fraction, image registration between the MVCT and kVCT was performed

Table 1. General information of four lung cancer patients

Patient number	Gender	Age (y)	Fraction number	Fraction dose (cGy)	Has 2nd phase
1	Male	92	30	200	No
2	Male	67	25	200	No
3	Female	77	20	250	No
4	Male	80	25	200	Yes

https://doi.org/10.1017/S1460396909990240 Published online by Cambridge University Press

using an automatic registration function in Planned Adaptive. Woodford et al.[5] suggested that with the selection of full image fusion and fine resolution will result in a low residual error in most of the cases when modifying image registration of MVCT and kVCT for lung cancer patients treated with helical TomoTherapy.

Concept of biologically effective uniform dose ($\overline{\overline{D}}$)

The uniform dose that causes the same tumour control probability or normal tissue complication rate as the actual dose distribution given to the patient was evaluated using the biologically effective uniform dose, $\overline{\overline{D}}$ (ref. 9,13). The general definition of the $\overline{\overline{D}}$ can be expressed as the equation below:

$$P\left(\overline{\overline{D}}\right) = P\left(\overrightarrow{D}\right), \quad (1)$$

where the $\overrightarrow{D}$ denotes the three-dimensional dose distribution.

The radiobiological model that was used to describe the dose-response relation of tumours and organs at risk was the linear-quadratic Poisson model[14,15]:

$$P(D) = \exp\left\{-N_0 e^{(D/D_{50})(e\gamma - \ln\ln 2)}\right\} = \exp\left\{-e^{e\gamma - \alpha nd - \beta nd^2}\right\}, \quad (2)$$

where the $P(D)$ is the probability to control the tumour or induce a certain injury to an organ that is irradiated uniformly with a dose D. Since this model takes into account the fractionation effects that are introduced by the irradiation schedule, d (equals to D/n) is the dose per fraction and n is the number of fractions. D_{50} is the dose which gives a response probability of 50% and γ is the maximum normalised value of the dose-response gradient. Variables α and β are the fractionation parameters of the model and account for the early and late effects, respectively. The dose-response parameters of the target and organs at risk used in this study are listed in Table 2.

$\overline{\overline{D}}_B$ is the biologically effective uniform dose, which is calculated based on the radiological characteristics of the target and it is associated with the clinical benefit. $\overline{\overline{D}}_I$ is the biologically effective uniform dose, which is calculated based on the radiological characteristics of normal tissues and it is associated with the radiation-induced injury.[9]

Table 2. Dose-response parameters used in biologically dosimetric evaluation

	D_{50} (Gy)	γ	s	α/β	End point
Spinal cord	57.0	6.70	1.00	3.0	Myelitis necrosis
Lungs	30.1	0.97	0.01	3.0	Severe radiation pneumonitis, fibrosis
Target	49.2	1.00	–	10.0	Control

D^{50} is the 50% response dose, γ is the maximum normalised value of the dose-response gradient and s is the relative seriality, which characterises the volume dependence of the organ.

Statistical methods for results

For four lung cancer patients, the physical doses to the target and critical organs were evaluated through the DVH at the prescription dose level for all treatment plans. The physical dose distributions were also calculated through the Planned Adaptive software for every five treatment fractions of the whole treatment course to periodically monitor the delivered dose distributions and to compare the measured dose distributions with the planned ones.[7] Based on the physical dose distributions, the DVHs and the dose-response parameters of the target and the critical organs of the treatment plans and actual delivered fractions, the $\overline{\overline{D}}$, tumour control probability (P_B), normal tissue injury rate (P_I) and complication-free tumour control probability (P_+) were determined for these four lung cancer patients.[9] Biological evaluations also included the assessment of the optimal $\overline{\overline{D}}$ and P_+ for all the treatment plans to indicate the ideal complication-free tumour control probability. The optimal P_+ is the maximum of the probability distribution calculated based on the $\overline{\overline{D}}$ (ref. 9). Additionally, the ratio of the delivered and the planned physical dose, biological doses and P_+ were calculated to show the efficiency of the TomoTherapy delivery physically and biologically.

Among these four patients, patient 4 had a two-phase treatment. In the first-phase treatment, because of the obvious tumour shrinkage

https://doi.org/10.1017/S1460396909990240 Published online by Cambridge University Press

observed in the planning target volume through the daily MVCT scans and the high cumulative dose to the ipsilateral lung, the physician decided to reduce the sizes of the irradiating fields and prescribe a second-phase plan after 16 fractions of TomoTherapy. The second-phase treatment of the patient 4 in this situation could be deemed as adaptive TomoTherapy. In order to get enough sampling points for the two-phase TomoTherapy of patient 4, the treatment plan and the actual delivered fractions were sampled for every two to five fractions instead of every five fractions.

RESULTS

Figure 1 demonstrates the ratio between the delivered and the planned physical doses to the target, that ratio calculated using the biologically effective uniform doses ($\overline{\overline{D}}_B$) and the ratio obtained by dividing the delivered to the planned P_+ for these four patients. Tables 3–6 summarise the physical mean dose ($\overline{D}$), $\overline{\overline{D}}_B$, $\overline{\overline{D}}_I$, P_+, P_B and P_I, which were calculated based on the treatment plans and the corresponding delivered fractions for patient 1 to patient 4. These tables also indicate the optimum (in the first column) of the biologically effective uniform dose and the complication-free tumour control rate for the treatment plan of each patient.

From Figure 1a, up to 9% under-dosage of the target is observed from the ratio of the delivered to the planned physical dose over a total of 30 treatment fractions (range from

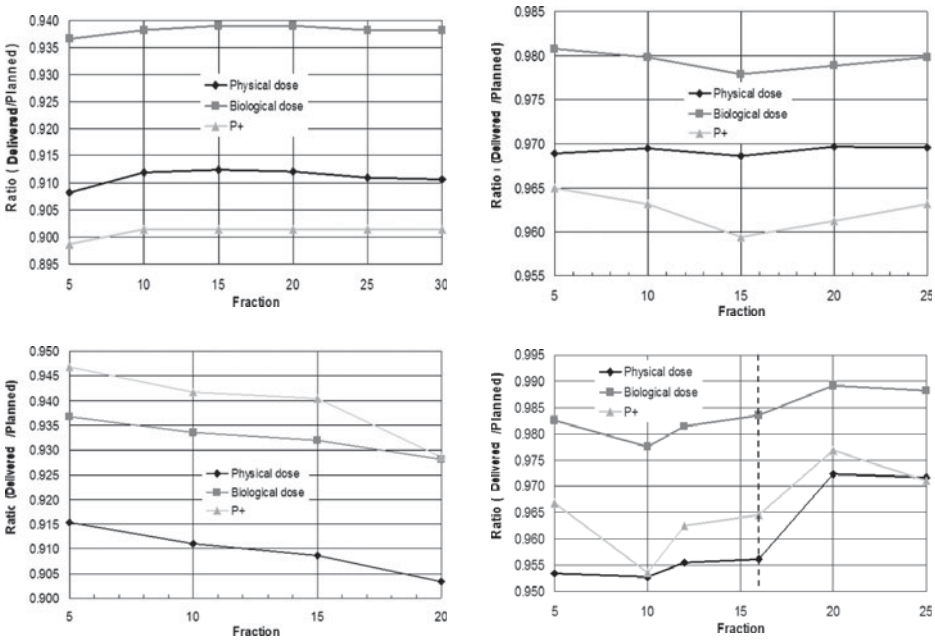

Figure 1. The ratios of the delivered to planned value in terms of physical dose, biological dose ($\overline{\overline{D}}$) and P_+

Table 3. *Summary of the radiobiological measures for the original treatment plan and delivered fractions of helical tomotherapy for patient 1*

	Optimum	Plan	5fx	10fx	15fx	20fx	25fx	30fx
$\overline{D}$ (Gy)	–	60.00	54.50	54.72	54.72	54.72	54.66	54.66
$\overline{\overline{D}}_B$(Gy)	89.00	60.65	56.80	56.90	56.95	56.95	56.90	56.90
$\overline{\overline{D}}_I$(Gy)	18.00	11.80	11.05	11.00	11.00	11.00	11.00	11.00
P_+	0.922	0.711	0.639	0.641	0.641	0.641	0.641	0.641
P_B	0.964	0.714	0.641	0.643	0.644	0.644	0.643	0.643
P_I	0.042	0.004	0.003	0.003	0.003	0.003	0.003	0.003

https://doi.org/10.1017/S1460396909990240 Published online by Cambridge University Press

Table 4. Summary of the radiobiological measures for the original treatment plan and delivered fractions of helical tomotherapy for patient 2

	Optimum	Plan	5fx	10fx	15fx	20fx	25fx
$\overline{D}$ (Gy)	–	50.00	48.45	48.45	48.45	48.50	48.50
$\overline{\overline{D}}_B$(Gy)	67.95	52.05	51.05	51.00	50.90	50.95	51.00
$\overline{\overline{D}}_I$(Gy)	21.25	15.90	15.40	15.35	15.30	15.35	15.35
P_+	0.721	0.542	0.523	0.522	0.520	0.521	0.522
P_B	0.847	0.566	0.543	0.542	0.539	0.540	0.541
P_I	0.125	0.024	0.020	0.019	0.019	0.019	0.019

Table 5. Summary of the radiobiological measures for the original treatment plan and delivered fractions of helical tomotherapy for patient 3

	Optimum	Plan	5fx	10fx	15fx	20fx
$\overline{D}$ (Gy)	–	50.00	45.75	45.55	45.45	45.15
$\overline{\overline{D}}_B$(Gy)	70.00	63.25	59.25	59.05	58.95	58.70
$\overline{\overline{D}}_I$(Gy)	19.45	17.35	15.95	15.95	15.90	16.25
P_+	0.799	0.771	0.730	0.726	0.725	0.716
P_B	0.897	0.822	0.760	0.757	0.754	0.750
P_I	0.098	0.051	0.030	0.030	0.030	0.034

Table 6. Summary of the radiobiological measures for the original treatment plan and delivered fractions of helical tomotherapy for patient 4

	Phase 1						Phase 2			
	Optimum	Plan	5fx	10fx	12fx	16fx	Optimum	Plan	20fx	25fx
$\overline{D}$ (Gy)	–	50.00	47.65	47.65	47.75	48.60	–	50.00	48.60	48.60
$\overline{\overline{D}}_B$(Gy)	62.00	51.30	50.40	50.15	50.35	50.45	74.00	50.55	50.00	49.95
$\overline{\overline{D}}_I$(Gy)	24.25	20.25	20.00	19.95	20.00	20.05	20.75	13.95	13.90	13.85
P_+	0.526	0.452	0.437	0.431	0.435	0.436	0.794	0.519	0.507	0.504
P_B	0.766	0.549	0.527	0.521	0.525	0.528	0.904	0.530	0.517	0.515
P_I	0.240	0.097	0.090	0.089	0.090	0.091	0.110	0.011	0.011	0.011

0.908 to 0.912). When evaluating the ratio between the delivered $\overline{\overline{D}}_B$ divided by the planned $\overline{\overline{D}}_B$, which was derived with the consideration of the biological characteristics of the target,[9,13] the biologically effective uniform dose that was delivered to the target is lower up to about 6%. These inferior ratios (range from 0.937 to 0.939) of $\overline{\overline{D}}_B$ over 30 fractions result in up to 10% lower P_+ compared to the planned P_+ throughout the treatment course of patient 1. According to Table 3, the optimal $\overline{\overline{D}}_B$ is 89.00 Gy and the optimal $\overline{\overline{D}}_I$ is 18.00 Gy, resulting in a P_+ of 92.2%.

In Figure 1b, the results of patient 2 show that the ratio of the delivered dose range from 0.969 to 0.970 in comparison with the planned prescribed dose. This results in deviations in $\overline{\overline{D}}_B$ from 0.978 to 0.981 over 25 treatment fractions of this patient. As a result, up to 4% lower P_+ compared to that of the treatment plan is observed during the treatment course. According to Table 4, the optimal $\overline{\overline{D}}_B$ of the treatment plan for patient 2 is 67.95 Gy and the optimal $\overline{\overline{D}}_I$ is 21.25 Gy, resulting in a P_+ of 72.1%.

For patient 3, the ratios between the delivered and the planned dose to the target range from 0.903 to 0.915 in 20 treatment fractions, resulting in ratios between 0.928 and 0.937 of the delivered $\overline{\overline{D}}_B$ to the planned $\overline{\overline{D}}_B$ as shown in Figure 1c. Furthermore,

https://doi.org/10.1017/S1460396909990240 Published online by Cambridge University Press

according to Figure 1c, up to 7% lower P_+ is observed at the end of 20th fraction for patient 3. Table 5 demonstrates that the optimal $\overline{\overline{D}}_B$ of the treatment plan for patient 3 is 70.00 Gy and the optimal $\overline{\overline{D}}_I$ is 19.45 Gy, resulting in a P_+ of 79.9%.

Figure 1d shows the results of patient 4, who had a second-phase treatment after the 16th of 30 treatment fractions. In the first-phase treatment, the ratio of the physical dose range from 0.953 to 0.956, which results in the ratio of the $\overline{\overline{D}}_B$ to vary from 0.978 to 0.983. As a result, up to 4.5% lower P_+ was calculated in the first-phase delivery of patient 4. In the second-phase treatment, the ratio of the physical dose increased to the values of 0.972 and the ratio of the $\overline{\overline{D}}_B$ rose up to 0.989. Therefore, the ratio of the P_+ grew up to 0.977 in the second-phase delivery. In Table 6, the optimal $\overline{\overline{D}}_B$ of 62.00 Gy, the optimal $\overline{\overline{D}}_B$ of 24.25 Gy and the P_+ of 52.6% for the first-phase treatment, and the optimal $\overline{\overline{D}}_B$ of 74.00 Gy, the optimal $\overline{\overline{D}}_I$ of 20.75 Gy and the P_+ of 79.4% for the second-phase treatment are listed.

Figure 2 shows the changes in terms of P_+ within the first-phase and the second-phase treatments and between the two treatment phases of patient 4. The P_+ of the second-phase treatment is significantly higher by about 13.2% as compared to the average P_+ in the first-phase treatment. On the other hand, the variation among the treatment fractions in terms of P_+ in the first-phase treatment is small. Also, there was no considerable change in P_+ within the second-phase treatment. The substantial increased P_+ in the second-phase TomoTherapy in comparison with the first-phase treatment indicates the clinical benefits of adaptive TomoTherapy for this lung patient.

DISCUSSION

Helical TomoTherapy of four lung cancer patients has been evaluated comprehensively using the Planned Adaptive software as well as the biologically effective uniform dose. In addition to the dosimetric evaluation, which is based on DVH and dose statistics (e.g. mean dose) obtained from the Planned Adaptive module, $\overline{\overline{D}}$ calculation was also employed to quantify

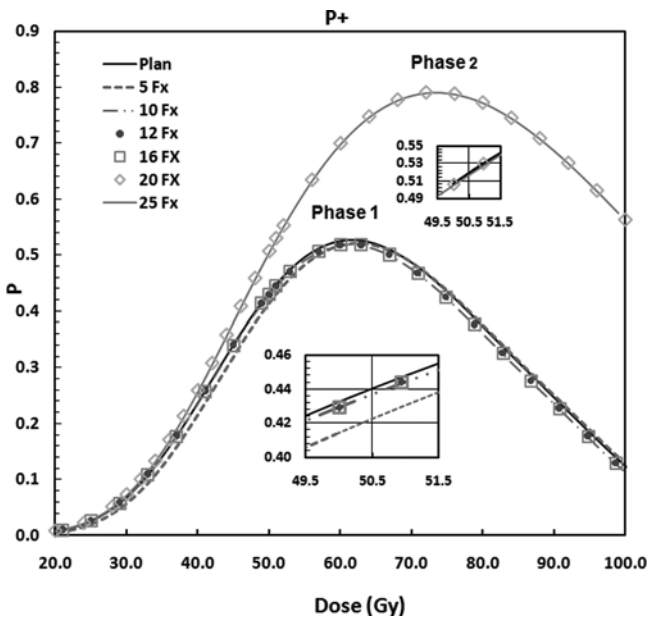

Figure 2. Variations of the P_+ in the first-phase and the second-phase treatment fractions. The subplots below the curves of the P_+ for these two phases showed the P_+ calculated based on the $\overline{\overline{D}}_B$ of the fractions (5th, 10th, 12th, 16th, 20th and 25th fractions) indicated in this figure.

https://doi.org/10.1017/S1460396909990240 Published online by Cambridge University Press

dose differences in terms of changes in the expected clinical outcome.[16] Quantification of the variation in tumour control probability and normal tissue complication rate for the delivered fractions would be more useful in adaptive planning during radiation therapy. The results in Figure 1 show the ratio of the delivered to the planned dose distributions in terms of the physical dose, the biological dose and the P_+. Over the whole course of treatment using TomoTherapy, the P_+ ratio curves revealed equal or more pronounced changes in comparison with the physical dose ratio curves for these four lung cancer patients. From Figure 1a,c, the clinical effect of different doses per fraction could be assessed by comparing results of patient 1 and patient 3. In Figure 1a,c, both curves of the physical dose ratios for patient 1 and patient 3, respectively, varied within a very similar range (in Figure 1a: 0.908−0.912; in Figure 1c: 0.903−0.915), indicating no significant difference ($p = 0.5950$). On the other hand, the P_+ ratios of patient 3, who had a larger dose-per-fraction, were significantly higher ($p = 0.0019$) than those of patient 1. The greater biological impact of the larger dose-per-fraction could be found[17,18] by using the P_+ evaluation, which was calculated with consideration of the dose-response parameters of the targets and organs at risk.

From the results in Figure 1 and Tables 3−6, the estimated doses delivered to the targets of the four lung cancer patients were different in trend. The same holds for the biologically effective uniform dose and complication-free tumour control rate over the whole course of treatment. Also, previous reports have proven that it is difficult to predict the volume changes in the target and treatment results based on the patient, treatment schedule or tumour characteristic.[4,6] Therefore, the individual evaluation of the dosimetric and clinical effects for each lung cancer patient treated with TomoTherapy using $\overline{\overline{D}}$ plus P_+ is necessary. Figure 1a shows the flat trends in the three curves of physical dose, biological dose and P_+ ratios after the 10th fraction (i.e., the 2nd week) of TomoTherapy for patient 1. The consistent suboptimal ratios over the whole treatment interval when compared to the treatment plan indicate the lack and, thus, the necessity of adaptive planning. The re-optimization of adaptive planning usually results in an improved tumour control probability combined with a limited normal tissue complication rate.[3] From the results of patient 2 in Figure 1b, it is shown that the decreasing trend of the P_+ ratios for the first 15 fractions contributed to the lowest complication-free tumour control rate observed at 15th fraction. The dosimetric evaluation of the Planned Adaptive software and the assessment of the clinical effects using the $\overline{\overline{D}}$ and the P_+ identify the dose deviations and, as a result, the lower P_+. With this information in the middle of the treatment, the physician could recheck the target contour, and the medical physicist could investigate the accuracy of dose delivery and the necessity of planning adaptation. For patient 3, the continuously decreasing ratios of the physical dose, the biological dose and the P_+ between delivered and planned dose distributions showed the suboptimal dose delivering of the treatment plan (cf. Figure 1c). With surveillance of physical doses and biological doses during TomoTherapy, the under-dosage of the target, resulting in lower tumour control, should be identified and corrected in time.

The results of patient 4 show the potential benefit of adaptive TomoTherapy as it is denoted by the significantly increased complication-free tumour control rate, resulting from the notably decreased normal tissue complication possibility. After the first-phase TomoTherapy (16 fractions), the physician decided to have a second-phase plan because of the considerably reduced tumour volume observed from the daily MVCTs and the high dose to the ipsilateral lung. From Figure 1d and Table 6, the P_+ ratios of the second-phase treatment (from 17th fraction to the end) increased by 1.2% as compared to the P_+ ratios of the first-phase treatment. When comparing the P_+ of the two treatment phases, P_+ of the second-phase TomoTherapy increased by 13.2% to the P_+ of the first-phase TomoTherapy. The reason for this significant increase in P_+ was mainly due to the notably lower P_I (8.6%) of the treatment plan in the second-phase treatment. The results of patient 4 with adaptive TomoTherapy are in line with the findings of Woodford et al.[4] Woodford et al.[4] suggested that adaptive planning

https://doi.org/10.1017/S1460396909990240 Published online by Cambridge University Press

can yield significant improvements in cumulative doses to organs at risk if the gross tumour volume decreases considerably. More evaluations are required on the need for adaptive planning especially for the cases in which the organs at risk impose significant dose limitation.[4] In comparison to previous reports,[4,6] our results not only show the changes in tumour volume with respect to the dosimetric effects when using the Planned Adaptive software, but it also demonstrate the increased tumour control rate and, thus, the escalating clinical effectiveness of the adaptive planning during the treatment course of TomoTherapy by using the $\overline{\overline{D}}$. Several studies have suggested the benefits of adaptive TomoTherapy by using the Planned Adaptive software to monitor the tumour volume changes and the margins around the tumour during the course of treatment.[4,8,19] In this study, the use of the $\overline{\overline{D}}$ leads to a closer association of the DVH and dose statistics with tumour control or normal tissue injury. With more information concerning the clinical impact of the delivered treatment, it would be possible to obtain a plan that is better tailored to the individual patient. For an adaptive schedule to be clinically feasible with respect to the clinical workload, the physicians could adjust the plan and the target coverage based on the predicted changes in complication-free tumour control rate at certain fractions. Therefore, the time and resources spent in re-planning would be justified by the increasing tumour control rate and/or decreasing normal tissue complication possibility.

Another advantage of the $\overline{\overline{D}}$ evaluation for the treatment plans and delivered fractions is the reports of the optimal P_+ calculated from the optimal compensation between the P_B and P_I indices. With the data of the optimal prescription level based on the tumour control probability and the normal tissue injury rate, it would be easier to pick up the optimal treatment plans before the treatment and to monitor the difference in the P_+ between the actual delivered dose and the optimal amount. It is also important to assess the available therapeutic window in terms of tumour control and normal tissue injury probabilities when considering about the necessity of using the adaptive planning. From the results in Tables 3–6, comparing the optimum in the first columns to the rest of the columns, large gaps can be observed in the $\overline{\overline{D}}$ and the P_+ between the optimal situations and the treatment plans for all four lung cancer patients. Even larger differences in the $\overline{\overline{D}}$ and the P_+ were found between the optimums and the actually delivered radiation. With the pre-knowledge of the optimal level of the $\overline{\overline{D}}$ and the P_+, adaptive planning should be performed to maximise the tumour control probability for a clinically acceptable normal tissue complication rate.[3,9]

The under-dosage of the target evaluated by using the Planned Adaptive software was as large as over 9% in both patient 1 and patient 3. Possible reasons for the notable dose deviations evaluated by the Planned Adaptive software are set-up error, organ motion and errors due to the image registration. Han et al.[7] assessed the actual dose variation to the target and the critical organs of patients treated with TomoTherapy using the Planned Adaptive module. They concluded that with the daily set-up corrections using the MVCT image registration, the variation in the dose could be as large as 7.7% around the average dose. In our study, in order to minimise the errors generated during the image registrations that were done right before the treatment, automatic image registrations were performed again for each treatment fraction of each lung cancer patient. Woodford et al.[5] suggested the optimal way of the MVCT registration setting for thoracic cases on helical TomoTherapy. Our study adopted their MVCT registration setting, registering the MVCT with the kVCT using either coarse or fine spacing with full image fusion technique and fine resolution selection. According to the conclusion of Woodford et al.,[5] the residual errors with the applied MVCT registration setting would be small with negligible influence on the dose calculation. Deformable registration was not used in this study, but could be a valuable extension. With the deformable image registration, more accurate assignment of doses to all structures could be defined with more reliable DVHs.

https://doi.org/10.1017/S1460396909990240 Published online by Cambridge University Press

The biggest advantage it could endow is the ability to create adapted plans that compensate for under-dosage or over-dosage of the target or critical organs.[4] In this study, the actual adaptive plans for these lung cancer patients were not delivered. The closest one is the second-phase plan in the second-phase treatment of patient 4. The main purpose of this study is to evaluate the feasibility of using the $\overline{\overline{D}}$ calculation in addition to the Planned Adaptive software to predict the clinical effect of helical TomoTherapy for these lung cancer patients. Also, our study tends to demonstrate the potential clinical benefits of adaptive planning like the second-phase plan of patient 4 through the $\overline{\overline{D}}$ assessment. The actual protocol of doing adaptive planning using the Planned Adaptive software is out of the scope of this paper.

Another possible source of errors in the dose estimation using the Planned Adaptive software might be attributed to the merged CT image. Planned Adaptive software merged the MVCT and the kVCT images after image registration. This merged MVCT-kVCT image has the same slice spacing as the kVCT images and is created by inserting the registered MVCT in the proper location and filling the remaining slices with the kVCT (TomoTherapy Inc., Planned Adaptive Guide). For the dose calculation in the Planned Adaptive software, both kVCT and MVCT CT numbers would be converted to electron densities by using the CT number to electron density calibration curves, respectively. Although the uniformity and spatial resolutions of the MVCT images are comparable to that of the diagnostic CT images, the MVCT unit does not have the same performance characteristics as those of the diagnostic kVCT scanner. Investigations have been done on the stability of the CT number to electron density calibration curve for both MVCT and kVCT units.[20,21] Langen et al.[21] concluded that although the variation in the MVCT number is larger than that of the kVCT image, the resulting electron density difference and, thus, the dose deviation after converting electron density to dose are similar in magnitude for a 6 MV beam. Therefore, the possible dosimetric errors in the merged MVCT-kVCT images generated by the Planned Adaptive software should be within 2–3% (ref. 20,21).

CONCLUSION

The dosimetric impact and the clinical effect of the adaptive TomoTherapy have been evaluated using the Planned Adaptive software plus the $\overline{\overline{D}}$. The knowledge of the tumour control and normal tissue injury over the partial or whole course of helical TomoTherapy would help the physician evaluate the necessity of adaptive planning. Based on our results for lung cancer patients treated with helical TomoTherapy, it is necessary to have the individual assessment with the $\overline{\overline{D}}$ in addition to the physical dose evaluated by the Planned Adaptive software. In contrast to the physical dose assessment, the better biological effect of the use of larger dose-per-fraction can only be observed in the increase of P_+ using the $\overline{\overline{D}}$ evaluation. Moreover, significant increase in the P_+ by 13.2% in the adaptive TomoTherapy plan in one of the lung cancer patients indicates the clinical benefit of the adaptive planning. In conclusion, the protocol of periodical evolution of the delivered dose using the $\overline{\overline{D}}$ may be set to achieve the end points of higher tumour control probability and/or lower normal tissue complication probability upon the adaptive radiation therapy.

References

1. Mackie TR, Kapatoes J, Ruchala K, Lu W, Wu C, Olivera G, Forrest L, Tome W, Welsh J, Jeraj R, Harari P, Reckwerdt P, Paliwal B, Ritter M, Keller H, Fowler J, Mehta M. Image guidance for precise conformal radiotherapy. Int J Radiat Oncol Biol Phys 2003; 56:89–105.
2. Welsh JS, Lock M, Harari PM, Tomé WA, Fowler J, Mackie TR, Ritter M, Kapatoes J, Forrest L, Chappell R, Paliwal B, Mehta MP. Clinical implementation of adaptive helical tomotherapy: a unique approach to image-guided intensity modulated radiotherapy. Technol Cancer Res Treat 2006; 5:465–479.
3. Yan D, Vicini F, Wong J, Martinez A. Adaptive radiation therapy. Phys Med Biol 1997; 42:123–132.
4. Woodford C, Yartsev S, Dar AR, Bauman G, Van Dyk J. Adaptive radiotherapy planning on decreasing gross tumor volumes as seen on megavoltage computed tomography

https://doi.org/10.1017/S1460396909990240 Published online by Cambridge University Press

images. Int J Radiat Oncol Biol Phys 2007; 69:1316–1322.

5. Woodford C, Yartsev S, Van Dyk J. Optimization of megavoltage CT scan registration settings for thoracic cases on helical tomotherapy. Phys Med Biol 2007; 52: N345–N354.
6. Siker ML, Tomé WA, Mehta MP. Tumor volume changes on serial imaging with megavoltage CT for non-small-cell lung cancer during intensity-modulated radiotherapy: how reliable, consistent, and meaningful is the effect? Int J Radiat Oncol Biol Phys 2006; 66:135–141.
7. Han C, Chen YJ, Liu A, Schultheiss TE, Wong JY. Actual dose variation of parotid glands and spinal cord for nasopharyngeal cancer patients during radiotherapy. Int J Radiat Oncol Biol Phys 2008; 70:1256–1262.
8. Ramsey CR, Langen KM, Kupelian PA, Scaperoth DD, Meeks SL, Mahan SL, Seibert RM. A technique for adaptive image-guided helical tomotherapy for lung cancer. Int J Radiat Oncol Biol Phys 2006; 64:1237–1244.
9. Mavroidis P, Lind BK, Brahme A. Biologically effective uniform dose (D) for specification, report and comparison of dose response relations and treatment plans. Phys Med Biol 2001; 46:2607–2630.
10. Mavroidis P, Plataniotis GA, Górka MA, Lind BK. Comments on 'Reconsidering the definition of a dose-volume histogram' – dose-mass histogram (DMH) versus dose-volume histogram (DVH) for predicting radiation-induced pneumonitis. Phys Med Biol 2006; 51:L43–L50.
11. Mavroidis P, Ferreira BC, Shi C, Lind BK, Papanikolaou N. Treatment plan comparison between helical tomotherapy and MLC-based IMRT using radiobiological measures. Phys Med Biol 2007; 52:3817–3836.
12. Su FC, Mavroidis P, Swanson G et al. Treatment planning for prostate cancer: Biologically quantitative comparisons among conventional radiotherapy and three IMRT delivery techniques. Boston, MA: ASTRO 50th annual meeting, 2008.
13. Mavroidis P, Lind BK, Van Dijk J, Koedooder K, De Neve W, De Wagter C, Planskoy B, Rosenwald JC, Proimos B, Kappas C, Claudia D, Benassi M, Chierego G, Brahme A. Comparison of conformal radiation therapy techniques within the dynamic radiotherapy project 'Dynarad'. Phys Med Biol 2000; 45:2459–2481.
14. Källman P, Agren A, Brahme A. Tumour and normal tissue responses to fractionated non-uniform dose delivery. Int J Radiat Biol 1992; 62:249–262.
15. Ågren Cronqvist AK, Kallman P, Brahme A. Determination of the relative seriality of a tissue from its response to non-uniform dose delivery modeling. In: Baltas D (ed). Clinical Radiobiology. Albert-Ludwigs-University, 1994, p. 127.
16. Mavroidis P, Ferreira BC, Papanikolaou N, Svensson R, Kappas C, Lind BK, Brahme A. Assessing the difference between planned and delivered intensity-modulated radiotherapy dose distributions based on radiobiological measures. Clin Oncol (R Coll Radiol) 2006; 18:529–538.
17. Song W, Battista J, Van Dyk J. Limitations of a convolution method for modeling geometric uncertainties in radiation therapy: the radiobiological dose-per-fraction effect. Med Phys 2004; 31:3034–3045.
18. Song WY, Chiu B, Bauman GS, Lock M, Rodrigues G, Ash R, Lewis C, Fenster A, Battista JJ, Van Dyk J. Prostate contouring uncertainty in megavoltage computed tomography images acquired with a helical tomotherapy unit during image-guided radiation therapy. Int J Radiat Oncol Biol Phys 2006; 65:595–607.
19. Drabik DM, MacKenzie MA, Fallone GB. Quantifying appropriate PTV setup margins: analysis of patient setup fidelity and intrafraction motion using post-treatment megavoltage computed tomography scans. Int J Radiat Oncol Biol Phys 2007; 68:1222–1228.
20. Kilby W, Sage J, Rabett V. Tolerance levels for quality assurance of electron density values generated from CT in radiotherapy treatment planning. Phys Med Biol 2002; 47:1485–1492.
21. Langen KM, Meeks SL, Poole DO, Wagner TH, Willoughby TR, Kupelian PA, Ruchala KJ, Haimerl J, Olivera GH. The use of megavoltage CT (MVCT) images for dose recomputations. Phys Med Biol 2005; 50:4259–4276.

https://doi.org/10.1017/S1460396909990240 Published online by Cambridge University Press